

Accelerated Article Preview

Emerging climate impact on carbon sinks in a consolidated carbon budget

Received: 23 July 2025

Accepted: 23 October 2025

Accelerated Article Preview

Published online: 12 November 2025

Cite this article as: Friedlingstein, P. et al.

Emerging climate impact on carbon sinks in a consolidated carbon budget. *Nature*
<https://doi.org/10.1038/s41586-025-09802-5>
(2025)

Pierre Friedlingstein, Corinne Le Quéré, Michael O'Sullivan, Judith Hauck, Peter Landschützer, Ingrid T. Luijx, Hongmei Li, Auke van der Woude, Clemens Schwingshackl, Julia Pongratz, Pierre Regnier, Robbie M. Andrew, Dorothee C. E. Bakker, Josep G. Canadell, Philippe Ciais, Thomas Gasser, Matthew W. Jones, Xin Lan, Eric Morgan, Are Olsen, Glen P. Peters, Wouter Peters, Stephen Sitch & Hanqin Tian

This is a PDF file of a peer-reviewed paper that has been accepted for publication. Although unedited, the content has been subjected to preliminary formatting. *Nature* is providing this early version of the typeset paper as a service to our authors and readers. The text and figures will undergo copyediting and a proof review before the paper is published in its final form. Please note that during the production process errors may be discovered which could affect the content, and all legal disclaimers apply.

1 **Emerging climate impact on carbon sinks in a consolidated carbon budget**

2
3 Pierre Friedlingstein^{1,2}, Corinne Le Quéré³, Michael O’Sullivan¹, Judith Hauck^{4,5}, Peter
4 Landschützer⁶, Ingrid T. Luijkx⁷, Hongmei Li^{8,9}, Auke van der Woude⁷, Clemens
5 Schwingshackl¹⁰, Julia Pongratz^{9,10}, Pierre Regnier¹¹, Robbie M. Andrew¹², Dorothee C. E.
6 Bakker¹³, Josep G. Canadell¹⁴, Philippe Ciais¹⁵, Thomas Gasser^{15,16}, Matthew W. Jones³, Xin
7 Lan^{17,18}, Eric Morgan¹⁹, Are Olsen^{20,21}, Glen P. Peters¹², Wouter Peters^{7,22}, Stephen Sitch¹,
8 Hanqin Tian²³

9
10 ¹ Faculty of Environment, Science and Economy, University of Exeter, Exeter EX4 4QF, UK

11 ² Laboratoire de Météorologie Dynamique, Institut Pierre-Simon Laplace, CNRS, Ecole Normale
12 Supérieure, Université PSL, Sorbonne Université, Ecole Polytechnique, Paris, France

13 ³ Tyndall Centre for Climate Change Research, School of Environmental Sciences, University of
14 East Anglia, Norwich Research Park, Norwich, NR4 7TJ, UK

15 ⁴ Alfred-Wegener-Institut, Helmholtz-Zentrum für Polar- und Meeresforschung, Am
16 Handelshafen 12, 27570 Bremerhaven, Germany

17 ⁵ Faculty of Biology/Chemistry, Universität Bremen, Bremen, Germany

18 ⁶ Flanders Marine Institute (VLIZ), Jacobsenstraat 1, 8400 Ostend, Belgium

19 ⁷ Environmental Sciences Group, Dept of Meteorology and Air Quality, Wageningen University,
20 Wageningen, The Netherlands

21 ⁸ Helmholtz-Zentrum Hereon, Max-Planck-Straße 1, 21502 Geesthacht, Germany

22 ⁹ Max Planck Institute for Meteorology, Bundesstraße 53, 20146 Hamburg, Germany

23 ¹⁰ Department of Geography, Ludwig-Maximilians-Universität München, Luisenstr. 37, 80333
24 Munich, Germany

25 ¹¹ Department of Geoscience, Environment & Society-BGEOSYS, Université Libre de Bruxelles,
26 1050 Brussels, Belgium

27 ¹² CICERO Center for International Climate Research, Oslo, Norway

28 ¹³ Centre for Ocean and Atmospheric Sciences, School of Environmental Sciences, University of
29 East Anglia, Norwich Research Park, Norwich NR4 7TJ, UK

30 ¹⁴ CSIRO Environment, Canberra, ACT 2602, Australia

31 ¹⁵ Laboratoire des Sciences du Climat et de l'Environnement, LSCE/IPSL, CEA-CNRS-UVSQ,
32 Université Paris-Saclay, 91198 Gif-sur-Yvette, France

33 ¹⁶ International Institute for Applied Systems Analysis (IIASA), Schlossplatz 1, 2361 Laxenburg,
34 Austria

35 ¹⁷ Cooperative Institute for Research in Environmental Sciences (CIRES),
36 University of Colorado Boulder, Boulder, CO 80305, USA

37 ¹⁸ National Oceanic and Atmospheric Administration Global Monitoring Laboratory
38 (NOAA/GML), 325 Broadway R/GML, Boulder, CO 80305, USA

39 ¹⁹ Scripps Institution of Oceanography, University of California San Diego, La Jolla, CA 92093-
40 0244, USA

41 ²⁰ Geophysical Institute, University of Bergen, Allégaten 70, 5007 Bergen, Norway

42 ²¹ Bjerknes Centre for Climate Research, Bergen, Norway

43 ²² University of Groningen, Centre for Isotope Research, Groningen, The Netherlands

44 ²³ Center for Earth System Science and Global Sustainability, Schiller Institute for Integrated
45 Science and Society, Department of Earth and Environmental Sciences, Boston College,
46 Chestnut Hill, MA 02467, USA.

47 Abstract
48 Despite the adoption of the Paris Agreement ten years ago, fossil CO₂ emissions continue to rise,
49 pushing atmospheric CO₂ levels to 423 ppm in 2024 and driving human-induced warming to
50 1.36°C, within years of breaching the 1.5°C limit ^{1,2}. Accurate reporting of anthropogenic and
51 natural CO₂ sources and sinks is a prerequisite to tracking the effectiveness of climate policy and
52 detecting carbon sink responses to climate change. Yet notable mismatches between reported
53 emissions and sinks have so far prevented confident interpretation of their trends and drivers ¹.
54 Here, we present and integrate recent advances in observations and process understanding to
55 address some long-standing issues in the global carbon budget estimates. We show that the
56 magnitude of the natural land sink is substantially smaller than previously estimated, while net
57 emissions from anthropogenic land-use change are revised upwards ¹. The ocean sink is 15%
58 larger than the land sink, consistent with new evidence from oceanic and atmospheric
59 observations ^{3,4}. Climate change reduces the efficiency of the sinks, particularly on land,
60 contributing 8.3 ± 1.4 ppm to the atmospheric CO₂ increase since 1960. The combined effects of
61 climate change and deforestation turn Southeast Asian and large parts of South American
62 tropical forests from CO₂ sinks to sources. This underscores the need to halt deforestation and
63 limit warming to prevent further loss of carbon stored on land. Improved confidence in
64 assessments of CO₂ sources and sinks is fundamental for effective climate policy.

65 The increase in atmospheric CO₂ concentration has been systematically monitored since the late
66 1950s, marking the beginning of comprehensive research into the global carbon cycle⁵. It soon
67 became evident that the observed increase in atmospheric CO₂ was smaller than the CO₂
68 emissions from burning fossil fuels, indicating that terrestrial ecosystems and/or the ocean acted
69 as carbon sinks⁶. Until the late 1980s, it was believed that the ocean was the main sink of
70 carbon, while the role of land ecosystems was unclear and was often referred to as the “missing
71 sink”⁷. The presence of a large CO₂ sink on land was confirmed later on, supported by field
72 studies⁸, biomass inventories⁹ or vegetation modelling¹⁰. Over the last 20 years, our
73 understanding of the global carbon cycle has rapidly improved, supported by the annual
74 assessments of the global carbon budget (GCB) activity of the Global Carbon Project. This
75 activity has enabled continuous community review of the anthropogenic perturbation on the
76 global carbon cycle^{1,11}. The GCB assessments are widely used in science and policy, including
77 in the latest assessment of the Intergovernmental Panel on Climate Change (IPCC)¹².

78

79 The carbon balance among individual components of the global carbon cycle provides a rigorous
80 test of our understanding of the carbon cycle: mass conservation implies that estimated net
81 emissions from fossil (EFOS) and land-use change (ELUC) and uptake by the ocean and land sinks
82 (SOCEAN and SLAND) must balance the observation-based atmospheric CO₂ growth rate GATM
83 perfectly. This has not been the case throughout the history of the GCB reports, including in the
84 latest 2024 update¹³ (hereafter GCB2024). GCB2024 reported a budget imbalance (B_{IM}; B_{IM}=
85 EFOS + ELUC - SLAND - SOCEAN - GATM) over the last decade of -0.4 ± 1.4 GtC/yr, which is about
86 10% of the observation-based atmospheric CO₂ growth rate. Despite its large uncertainty, the
87 negative B_{IM} implies that estimated sources were too low and/or estimated sinks too large. Over
88 the last 65 years, the B_{IM} also showed a negative trend of -0.14 ± 0.04 GtC/yr per decade,
89 statistically significant at the 1% level (p-value=0.003), with a positive B_{IM} in the early part of
90 the record and a negative B_{IM} in the most recent years (Extended Data Fig. 1).

91

92 A statistically significant trend in the B_{IM} impedes robust interpretation of trends in individual
93 components of the global carbon budget. Hence, reducing the magnitude and trend of the B_{IM} is a
94 prerequisite to reliably assessing temporal changes in the strength of the carbon sinks. Here, we
95 present and integrate recent advances in observations and process understanding to improve our

96 estimates of components of the global carbon budget, with direct impact on the magnitude and
97 trend of the B_{IM} . These improvements allow a more robust assessment of the human interference
98 on the global carbon cycle over the past 65 years, and of the emerging impacts of climate change
99 on the evolution of the carbon sinks.

100

101 **Introducing the latest evidence**

102 The net land-use change CO₂ emissions (ELUC) assessed in the GCB are derived from
103 bookkeeping models forced by reported changes in land use. Most bookkeeping models assume
104 that land-cover types, such as forest or pasture, have distinct but static equilibrium carbon
105 densities (i.e., amount of carbon per unit area of a full-grown ecosystem)¹³. This assumption
106 allows to isolate the direct land-use impact (e.g., due to deforestation, afforestation) from indirect
107 human-induced effects on vegetation^{14,15} such as higher global biomass and higher soil carbon
108 densities due to environmental effects (e.g., due to atmospheric CO₂ increase)¹⁶. However,
109 neglecting the effects of environmental changes in ELUC estimates results in an underestimation
110 of the historical ELUC trend^{16,17}. To address this issue, we replaced the static carbon densities
111 used in bookkeeping models by transient values informed by dynamic global vegetation models
112 (DGVMs) derived carbon dynamics^{17,18} (see Methods). Accounting for transient carbon
113 densities leads to an increase in net ELUC of 0.11 ± 0.04 GtC/yr over the last decade, and
114 additional emissions of 3.0 ± 1.0 GtC since 1960 (Fig. 1a and Extended Data Fig. 2b).

115

116 The land CO₂ sink (S_{LAND}) is estimated in GCB from DGVMs using historical simulations that
117 assume a constant pre-industrial land cover. In doing so, the models do not double account for
118 CO₂ fluxes associated with land-cover changes from anthropogenic land use, which are already
119 included in ELUC. However, given the historical reduction in forest cover and expansion of
120 agriculture, assuming a pre-industrial land cover leads to an overestimation of the land sink^{17–20}.
121 This is a known bias now referred to as the Replaced Sinks and Sources (RSS)^{17,19,21}. To address
122 this issue, we developed a new correction method using outputs from the DGVMs that resolve
123 net land-atmosphere carbon fluxes at the plant functional type level (see Methods). Accounting
124 for evolving land-cover change leads to a decrease of the mean S_{LAND} by 0.5 ± 0.3 GtC/yr over
125 the last decade, and a decrease of 21 GtC since 1960 (Fig. 1b and Extended Data Fig. 3d).

126

127 The land and ocean CO₂ sinks in the GCB account for the lateral carbon export (LCE) from land
128 ecosystems to inland waters, coastal environments, and the open ocean using natural (pre-
129 industrial) estimates of 0.65 ± 0.30 GtC/yr^{22,23} but neglecting its anthropogenic perturbation.
130 Recent advances in understanding aquatic carbon cycle processes indicate an increase in carbon
131 exported from terrestrial ecosystems to the aquatic environment, with an increased outgassing of
132 CO₂ from these aquatic systems to the atmosphere, increased carbon storage in aquatic sediments
133 and export to the ocean^{24,25} (see Methods). Accounting for the anthropogenic perturbation of
134 LCE leads to a decrease of the mean S_{LAND} by 0.07 ± 0.06 GtC/yr over the last decade (Fig. 1b
135 and Extended Data Fig. 3).

136

137 The ocean CO₂ sink in the GCB combines independent estimates from data products based on
138 observations (fCO₂-products)^{26,27} as well as global ocean biogeochemical models (GOBMs).
139 fCO₂-products and GOBMs broadly agree on ocean sink trends and variability, with remaining
140 differences mostly explained by limited data and seasonal biased sampling causing
141 overestimation in decadal trends of fCO₂-products, and possible GOBM underestimation of
142 decadal variability²⁸, especially in the Southern Ocean^{29–31}. However, fCO₂-products suggest a
143 substantially larger ocean sink than GOBMs (3.1 ± 0.3 GtC/yr versus 2.6 ± 0.4 GtC/yr,
144 respectively, over 2014–2023), which is also supported by independent constraints derived from
145 atmospheric CO₂ and oxygen observations³ as well as ocean interior observations⁴. Multiple
146 model evaluation efforts have now shown that GOBMs underestimate the mean oceanic sink in
147 the order of 10%, based on evidence of too weak overturning circulation³², ocean interior
148 constraints³³, and biases arising from spin-up strategies³⁴. In parallel, estimates from fCO₂-
149 products could also be biased low because they do not account for temperature gradients between
150 the measurement depth, usually several meters below surface, and the surface skin layer where
151 the gas exchange takes place^{35–37}. Accounting for the GOBMs bias and for skin temperatures
152 and warm layer in fCO₂-products leads to an increased S_{OCEAN} of 0.2 ± 0.23 GtC/yr over the last
153 decade, and an increase of 11 ± 14 GtC since 1960 (Fig. 1c and Extended Data Fig. 2c).

154

155 Fossil CO₂ emissions (EFOS) include the oxidation of fossil fuels from combustion, chemical
156 reactions, decomposition of fossil carbonates, and the CO₂ uptake from the cement carbonation¹.
157 The GCB estimate of EFOS (9.7 ± 0.5 GtC/yr for the 2014–2023 period) is a composite of

158 different datasets, aimed to give the best emission estimate and reduce biases. The differences
159 between independent datasets are well understood, with the range between different datasets
160 around 5% and with all showing similar trends ³⁸. EFOS misses minor emission sources in some
161 developing countries for decomposition of some carbonates, estimated to be <0.5% of the global
162 total. The cement carbonation sink is probably the most poorly constrained element of EFOS, but
163 at 0.2 GtC/yr in recent years, the contribution to EFOS uncertainty is small. Hence, we do not
164 have any compelling reason to suspect a substantial bias in global EFOS mean or trend that would
165 require a correction in this study.

166

167 The atmospheric CO₂ growth rate (G_{ATM}) in GCB is based on marine boundary layer CO₂ mole
168 fraction observations (in ppm/yr), which have only a small measurement uncertainty ³⁹. These
169 measurements are subsequently converted to mass growth rates in GtC/yr using a conversion
170 factor (CF), which so far has been assumed to be a constant value of 2.124 GtC/ppm, without
171 associated uncertainty ⁴⁰. However, the surface fluxes that lead to changes in atmospheric mole
172 fractions are not instantaneously observed at the surface stations, given that atmospheric mixing
173 takes time. The surface network is also not fully representative of the whole atmosphere ⁴¹. Any
174 variability and uncertainty in CF would propagate into the estimated annual CO₂ growth rate
175 (G_{ATM}) and its uncertainty. Here we quantify the annual CF values and their uncertainties using
176 the atmospheric inversions from the GCB (see Methods). In Extended Data Fig. 4, we show
177 these CFs and the resulting uncertainty on G_{ATM} and the B_{IM}. Including annually varying CFs
178 would mainly reduce the variability of the B_{IM} (up to 40%) but has no effect on its mean or trend.
179 This interannual effect of CF will be further evaluated and considered for inclusion in future
180 GCB assessments.

181

182 **Consolidating the global carbon budget**

183 The inclusion of known missing processes and the associated corrections on ELUC, SLAND and
184 SOCEAN in the GCB2024 estimate ¹ results in a consolidated global carbon budget (Table 1, see
185 also Extended Data Table 1 and 2). The revised estimate of ELUC, when accounting for transient
186 carbon densities, is 1.2 ± 0.7 GtC/yr for the last decade (2014-2023). Although the correction
187 increases land-use change emissions with time, the statistically significant decline in ELUC of
188 0.2GtC/decade since the late 1990s, as identified in GCB2024, remains (p-value<0.001). About

189 75% of the 0.11 ± 0.04 GtC/yr increase in E_{LUC} is due to larger net land-use change emissions in
190 South America, Southeast Asia, and Africa. Note that while the net effect of anthropogenic land-
191 use change is a source of CO₂ to the atmosphere, parts of the world including North America,
192 Europe, and China are currently net carbon sinks from land-use change. Total global
193 anthropogenic net CO₂ emissions ($E_{FOS}+E_{LUC}$) increased until the 2000s but remained relatively
194 constant after 2010 at around 11 GtC/yr.

195

196 S_{LAND} is substantially reduced when accounting for evolving land-cover change and for the
197 increase in terrestrial carbon outgassed by inland waters. The revised mean land sink is 2.7 ± 0.9
198 GtC/yr over 2014-2023 (Fig. 1b, Table 1). As a result, the revised net land CO₂ flux ($S_{LAND} -$
199 E_{LUC}) is reduced by 31% from a sink of 2.1 ± 1.1 GtC/yr to a sink of 1.4 ± 1.1 GtC/yr (Table 1).
200 Conversely, the revised ocean CO₂ sink is increased by 8% when accounting for the effect of
201 warm layer and cool skin on ocean fCO₂ products and correcting for the known GOBMs bias,
202 reaching 3.1 ± 0.5 GtC/yr over the past decade (Fig. 1c, Table 1). As a result of these revisions,
203 the ocean sink is about 15% larger than the land sink while it was 10% lower in GCB2024 (Table
204 1), although these differences remain within the uncertainty bounds of both fluxes.

205

206 The corrections applied to E_{LUC} , S_{LAND} and S_{OCEAN} are each within the uncertainty of the initial
207 estimates, hence the revised estimates are not statistically significantly different from the
208 GCB2024 estimates (Table 1). However, the corrections applied here are based on known
209 biogeochemical processes, which have not been considered in the GCB estimates so far.
210 Furthermore, high confidence can be placed on the sign of each of these corrections: assuming
211 constant vegetation densities leads to an underestimation of E_{LUC} , assuming pre-industrial land
212 cover leads to an overestimation of S_{LAND} , ignoring historical increase in lateral carbon export
213 also leads to an overestimation of S_{LAND} , and neglecting the ocean cool skin effect leads to an
214 underestimation of S_{OCEAN} . Hence the revised estimate of E_{LUC} , S_{LAND} and S_{OCEAN} represents an
215 improvement in their representation in the global carbon budget. Furthermore, the revised
216 budget, with a smaller net land CO₂ (1.4 ± 1.2 GtC/yr) and a larger ocean sink (3.1 ± 0.5
217 GtC/yr), is fully consistent with the estimates from atmospheric inversions (1.4 ± 0.5 GtC/yr and
218 3.1 ± 0.5 GtC/yr for the net land flux and the ocean sink, respectively), and with estimates
219 derived from atmospheric O₂ observations (1.0 ± 0.8 GtC/yr and 3.4 ± 0.5 GtC/yr, respectively)

220 (Table 1)^{1,3,42}. The convergence of these independent estimates gives stronger confidence that
221 this revised budget provides more robust estimates compared to GCB2024.

222 The budget imbalance, which was -0.4 ± 1.3 GtC/yr over 2014-2023 in GCB2024, is reduced to
223 near zero (-0.1 ± 1.3 GtC/yr) (Fig. 1d, Table 1), although it is not statistically significantly
224 different from the GCB2024 estimate. Finally, the statistically significant negative trend in the
225 BIM over the last 65 years of -0.14 ± 0.04 GtC/decade (p-value= 0.003) in the GCB2024 estimate
226 is now reduced to a non-significant trend of -0.06 ± 0.04 GtC/decade (p-value= 0.14), adding
227 confidence in the revised estimate of the global carbon budget presented here (Extended Data
228 Fig. 2f).

229

230 **Influence of climate change**

231 With virtually no imbalance, the consolidated global carbon budget provides a basis for
232 analysing the long-term evolution of the land and ocean sinks and their role in mitigating the
233 atmospheric CO₂ increase due to anthropogenic CO₂ emissions. Climate change is widely
234 expected to cause a reduction of CO₂-induced land and ocean carbon sinks (relative to a
235 theoretical case with the same atmospheric CO₂ increase but no climate change)^{12,43,44}. Using
236 additional historical simulations of GOBMs and DGVMs driven by the observed atmospheric
237 CO₂ increase but under a constant climate forcing (see Methods), we estimate that the effect of
238 climate change has reduced the land and ocean sinks by 0.8 ± 0.9 GtC/yr (-23%) and 0.18 ± 0.1
239 GtC/yr (-6%), respectively over the last decade (Fig. 2a,b and Fig. 3), with tropical regions
240 accounting for the largest effect on land (Fig. 4). The cumulative reduction in the land and ocean
241 sinks combined amounts to 30 ± 6 GtC (29 ± 6 GtC and 2 ± 1 GtC, respectively) since 1960,
242 implying that the carbon-climate feedback has already contributed 8.3 ± 1.4 ppm (8%) to the rise
243 in atmospheric CO₂ concentration (Fig. 2c).

244

245 The net land CO₂ flux can be decomposed in three contributions: the response to atmospheric
246 CO₂ increase, the response to climate change (e.g., temperature, rainfall), and land-use change
247 (Extended Data Fig. 5). Over the decade of 2014-2023, the atmospheric CO₂ increase induced a
248 3.6 ± 1 GtC/yr sink, while the effect of climate and land-use change led to a source of 0.9 ± 0.6
249 GtC/yr and 1.2 ± 0.7 GtC/yr, respectively, bringing the net land CO₂ flux to a sink of 1.4 ± 1.2

250 GtC/yr. The combined effect of climate change and land-use change is largest in the tropics.
251 While deforestation is the main driver of carbon losses in Africa and South-East Asia, climate
252 impacts on ecosystems are the dominant causes of carbon losses in South America (Fig. 4), in
253 line with observational evidence ^{45,46}. Our findings reinforce the need to halt deforestation and to
254 mitigate climate change to prevent an increasingly larger fraction of the terrestrial biosphere
255 from becoming a source of CO₂.

256

257 **Implications**

258 Recent advances in observations and understanding implemented here within the GCB have
259 contributed to addressing some of the long-standing issues and improving coherence between
260 bottom-up estimates from DGVMs and GOBMs and top-down estimates based on atmospheric
261 CO₂ inversions and O₂ observations. Important uncertainties remain, as reflected by the large
262 interannual variability still present in the B_{IM}, and global agreement between bottom-up and top-
263 down estimates could still be due to compensating errors in critical processes in components of
264 the global carbon budget. Further improvements are required in several areas, including on the
265 estimates of carbon losses from land degradation; the understanding of the long-term impact of
266 fires on carbon storage; the representation of small-scale physical processes in GOBMs; the
267 understanding of the variability of the biological ocean carbon pump; the Southern Ocean
268 observational coverage for better fCO₂-product representation; and the reconciliation of bottom-
269 up and top-down estimates at the regional level. Delivering on those issues hinges on continued
270 monitoring of atmospheric and surface ocean CO₂ levels, which are fundamental to carbon cycle
271 research. Maintaining regular assessments of the sources and sinks of CO₂ and integrating the
272 latest understanding will facilitate monitoring changes in the natural carbon cycle and lead to
273 more informed and effective decisions.

274 **Methods**

275

276 **Land-use change emissions. Transient carbon densities correction (δL)**

277 In the GCB, ELUC is estimated based on four bookkeeping models driven by historical land-use
278 change data. All but one of the bookkeeping models (OSCAR, see below) use static equilibrium
279 carbon density values for vegetation and soil from various sources, representative of “present-
280 day” carbon densities. The OSCAR bookkeeping model does not require any adjustment as it
281 already endogenously simulates changes in biome carbon densities under environmental
282 changes, in parallel to the bookkeeping calculation of ELUC^{18,47}. Although not used in GCB2024,
283 the BLUE bookkeeping model also offers alternative ELUC estimates based on transient carbon
284 densities¹⁷. To adjust for δL in BLUE, the static equilibrium carbon densities are converted into
285 transient densities based on the carbon density evolution from DGVMs from the GCB (under
286 simulations with transient environmental changes but constant land cover, termed S2, see
287 below). Transient biomass carbon densities are derived based on twelve DGVMs and transient
288 soil carbon densities based on seven DGVMs providing the necessary providing the necessary
289 plant functional type (PFT)-level output.

290 For the other two bookkeeping models that use static carbon densities in GCB2024 (H&C23 and
291 LUCE), the ELUC estimates under transient carbon densities are derived by scaling their ELUC
292 values with the average ratio of ELUC with transient densities to ELUC with static densities
293 estimated from OSCAR and from BLUE. Scaling is done individually for each of the following
294 ELUC sub-components: total deforestation, total forest (re-)growth, gross sources from wood
295 harvest, gross sinks from wood harvest, and other transitions. The resulting component-wise
296 ELUC with transient densities estimates are then summed to obtain the net ELUC estimate for
297 H&C23 and for LUCE. The uncertainty on δL is estimated based on uncertainty estimates from
298 BLUE and OSCAR. For BLUE, we estimate the δL uncertainty (one standard deviation) across
299 the estimates from the seven DGVMs providing PFT-level output for soil and vegetation carbon

300¹⁷. For OSCAR, the δL uncertainty is estimated as weighted standard deviation¹⁸. The δL
301 uncertainty for H&C23 and LUCE is derived as the average relative uncertainty of BLUE and
302 OSCAR. The final δL uncertainty is estimated using a random-effects model considering both
303 the uncertainty estimates of each model and the variability of δL estimates across bookkeeping

304 models. The transient carbon densities correction (δL) leads to an increase in E_{LUC} of 0.11 ± 0.04
305 GtC/yr for the last decade.

306

307 **Land sink. Replaced sinks and sources correction (RSS)**

308 In the GCB, the natural land sink (S_{LAND}) is estimated using simulations from an ensemble of
309 DGVMs that follow a common experimental protocol. Each model performs several simulations
310 in order to isolate drivers of changes in land carbon fluxes. S_{LAND} is estimated with the “S2”
311 simulation, where atmospheric CO₂ and climate vary over time, but land cover is held at pre-
312 industrial (year 1700) levels. This setup is designed to isolate the direct effects of rising CO₂,
313 climate change, and nitrogen deposition on land carbon uptake, while excluding effects of direct
314 human-driven land-use change. These latter are calculated separately in the E_{LUC} flux estimated
315 with the bookkeeping models. Because land cover is fixed at pre-industrial levels, these S2
316 simulations represent the response of the land surface to rising atmospheric CO₂, nitrogen
317 deposition, and changes in climate with too much forest cover globally (as forest area has
318 decreased by about 20% since 1700). As carbon sinks in forests are typically larger than in other
319 ecosystems, the S_{LAND} term is overestimated. This issue is known as the replaced sinks and
320 sources (RSS)^{17,19} (in some publications also called the loss of sink capacity²¹). To address this
321 issue, a recent study⁴⁸ developed a correction method that adjusts the S_{LAND} estimate to reflect
322 the actual historical land cover distribution while still excluding carbon fluxes associated with
323 direct human influences on land cover (e.g., from deforestation, af/reforestation). The method
324 uses a subset of seven DGVMs that simulate net biome production (NBP) at the PFT level and
325 include separate soil and litter carbon pools for each PFT. These models provide outputs from
326 both the S2 simulation and the S3 simulation (varying CO₂, climate, and land use/cover). We
327 extract the PFT-level NBP from the S2 simulation and combine it with the time-varying land
328 cover fractions from S3. This allows us to reconstruct a corrected NBP flux that reflects how the
329 land system would respond to CO₂ and climate under the actual, changing land cover, while
330 excluding anthropogenic land-use change emissions and sinks. We then compute the bias as the
331 difference between the original S_{LAND} (from the S2 simulation) and the reconstructed, land-
332 cover-corrected S_{LAND} . The global correction is derived by summing grid cell-level biases across
333 the models, and the uncertainty is estimated from the inter-model standard deviation. This
334 correction leads to a decrease of S_{LAND} by 0.5 ± 0.3 GtC/yr for the 2014-2023 period.

335

336 **Land sink. Lateral carbon export correction (LCE)**

337 In the GCB, the impact of human-induced changes in lateral carbon transfers on the land and
338 ocean carbon sinks and G_{ATM} have so far been excluded. Here, we account for anthropogenic
339 impacts on these lateral fluxes by taking the average of two recently published estimates: a data-
340 ensemble method ²⁴ and a process-based model which includes land-aquatic lateral exchanges
341 and CO_2 fluxes with the atmosphere ²⁵. The two estimates are quantitatively consistent, are
342 supported by a recent global assessment using another land surface model enabled for land-
343 aquatic lateral exchanges (H. Zhang, pers. com.), and are very close (within 10 %), for their
344 present-day carbon export estimate, to a recent global assessment relying on process-based
345 models, observations and machine learning ⁴⁹. Extended Data Fig. 3 provides an overview about
346 the different components of the carbon export correction. The anthropogenic perturbation (2014-
347 2023 minus pre-industrial) on the lateral land-to-inland water carbon flux (F'_{LI}) amounts to 0.54
348 ± 0.44 GtC/yr and is partitioned into increased aquatic CO_2 evasion (F'_{IA} , 0.34 ± 0.26 GtC/yr),
349 aquatic carbon storage (F'_{IS} , 0.09 ± 0.03 GtC/yr), and carbon exports to the ocean (F'_{IE} , $0.11 \pm$
350 0.08 GtC/yr).

351 To estimate the impact of this enhanced lateral carbon export on S_{LAND} , we use the process-based
352 estimate ²⁵ which allows to separate the lateral land-to-inland water carbon flux (F'_{LI}) depending
353 on the origin of the exported carbon. Incidentally, one half (0.27 ± 0.31 GtC/yr) results from the
354 transfer of dissolved CO_2 from the soil water column to the aquatic system, and the other
355 half (0.27 ± 0.31 GtC/yr) results from the transfer of terrestrial organic carbon to the aquatic
356 system. The former (numbers in orange in Extended Data Fig. 3) represents a lateral
357 displacement of CO_2 produced by soil heterotrophic respiration to the aquatic system (F'_{IA} ,
358 orange values), with no impact on the combined terrestrial+aquatic CO_2 flux to the atmosphere,
359 and hence no impact on S_{LAND} . The latter (numbers in red in Extended Data Fig. 4) represents an
360 additional loss from terrestrial ecosystems carbon reservoirs to the aquatic system, which can
361 impact S_{LAND} . Indeed, out of the 0.27 ± 0.22 GtC/yr of organic carbon lost from the terrestrial
362 reservoirs, about one quarter, 0.07 ± 0.06 GtC/yr, is transferred to inland waters, decomposed
363 and released back to the atmosphere as CO_2 , hence impacting S_{LAND} (F'_{IA} , red values), while the
364 remaining three quarters are stored in other reservoirs (0.09 ± 0.03 GtC/yr buried in aquatic
365 systems, F'_{IS} and 0.11 ± 0.08 GtC/yr exported to the open ocean, F'_{IE}), with no impact on S_{LAND} .

366 We do not correct the GCB estimate of the ocean sink (SOCEAN), i.e., we assume that the
367 terrestrial carbon exported to the ocean (F'_{IE} , 0.11 ± 0.08 GtC/yr GtC/yr) remains stored in the
368 ocean, as the fate of the land-derived carbon in the coastal and open ocean remains too uncertain
369 to be quantified with confidence ²⁴.

370 In summary, the lateral carbon export (LCE) correction leads to a 0.07 ± 0.06 GtC/yr reduction
371 of S_{LAND} , with the uncertainty estimated by combining the uncertainties reported in the original
372 studies for enhanced CO₂ outgassing ^{24,25}. No LCE correction on SOCEAN was applied here.

373

374 **Ocean sink bias correction**

375 In the GCB, the ocean carbon sink (SOCEAN) is calculated as the mean of the ensemble average of
376 global ocean biogeochemical models (GOBMs) and the ensemble average of observation-based
377 estimates (fCO₂-products). Both approaches are subject to known biases that are quantified here.

378 The evidence for the underestimation of the ocean CO₂ sink using GOBMs, already mentioned in
379 GCB2024 ¹ comes from a number of studies, which all suggest an underestimation of around
380 10%. Comparison with interior ocean estimates of anthropogenic carbon accumulation suggests
381 an underestimation of 8% ⁴ to 17% ³³ for the periods 1994-2007 and 2004-2014, respectively.

382 GOBMs produce a lower ocean sink compared to atmospheric inversions (by 16%) and
383 atmospheric oxygen-based estimates (by 24%), for the decade 2014-2023 ¹, although uncertainty
384 ranges overlap. Process-based evaluation of the Earth System Models (ESMs) also suggests a 9-
385 11% underestimation of the ocean sink due to biases in simulated Atlantic Meridional

386 Overturning Circulation, Southern Ocean ventilation, and surface ocean Revelle factor ⁵⁰, also
387 qualitatively supported by regional studies ⁵¹⁻⁵³. A composite analysis of GOBMs and ESMs
388 suggest that GOBMs underestimate the ocean sink by 10% due to inadequate spin up strategies
389 ³⁴. Regionally, eddy-covariance CO₂ flux data suggest a substantial underestimation of the

390 Southern Ocean sink by the GOBMs ⁵⁴. All in all, while all lines of evidence have their own
391 uncertainties, they consistently support that GOBMs underestimate the ocean sink. We thus have
392 high confidence (90% confident) that the correction on the GOBMs estimate is positive. Hence,
393 we propose a correction of $+10\% \pm 8\%$ based on the evidence provided above, with the
394 uncertainty consistent with a 90% chance the correction is positive (Z-score = -1.28). The upward

395 scaling of the GOBMs by 10% results in an increase of the GOBM sink estimate by 0.26
396 ± 0.21 GtC/yr for the 2014-2023 period.

397 Observation-based estimates (fCO₂-products) are built on direct measurements of the fugacity of
398 CO₂ (fCO₂, which equals pCO₂ corrected for the non-ideal behaviour of the gas) from the
399 Surface Ocean CO₂ Atlas (SOCAT)²⁶ that are gap filled using various statistical, regression and
400 machine learning approaches. The air-sea CO₂ exchange is then calculated from the air-sea
401 partial pressure difference of CO₂ and a wind dependent bulk gas transfer formulation. These
402 calculations do not consider temperature gradients arising from the surface warm layer and cool
403 skin effect (the less than 1 mm thick surface micro-layer that cools through ocean heat loss to the
404 atmosphere), which are mechanistically well understood but have historically been difficult to
405 quantify. A recent study based on field study of direct air-sea CO₂ fluxes suggests that the
406 measurements need to be adjusted to consider a cool skin effect (0.42 GtC/yr, increasing sink),
407 which is in part offset by the effect of temperature differences between the measurement depth
408 and the ocean surface (0.24 GtC/yr, decreasing sink), resulting in an upward adjustment of the
409 sink of 0.18 GtC/yr³⁷. This is broadly consistent in magnitude with a GOBM model study that
410 implemented the cool skin effect⁵⁵. For the cool skin and warm layer corrections of the fCO₂-
411 products, the field study estimate comes without uncertainty³⁷. However, based on the
412 uncertainty estimate of the modelling study⁵⁵ and our expert judgement, we have medium
413 confidence (66% confidence) that the correction is positive. Uncertainties remain, e.g. due to the
414 lack of dedicated field campaigns and choice of rapid or equilibration model for the cool skin
415 correction^{36,56}, and should be resolved in the future to increase confidence. Hence, we propose a
416 correction of 0.18 ± 0.4 GtC/yr, with the uncertainty consistent with a 66% chance the correction
417 is positive (Z-score = -0.45). Additional warm bias leading to potential enhanced underestimation
418 of the ocean sink has been identified also from variable sample depth and potential artificial
419 warming in the ship environment, but these factors are less well understood and constrained^{35,36}
420 and thus not further considered here.

421 In our revised assessment, we increase the GOBMs estimate by $10 \pm 8\%$ and the fCO₂-products
422 estimate by 0.18 ± 0.4 GtC/yr. These two corrections combined lead to an increase of SOCEAN by
423 0.22 ± 0.23 GtC/yr for the 2014-2023 period.

424 We note that the adjustment of both GOBM and fCO₂-product estimates does not resolve the
425 discrepancy between them, but it does align the GCB mean ocean sink closer to independent
426 estimates based on observations of the ocean interior and of atmospheric oxygen ^{3,4}

427

428 **Atmospheric CO₂ growth rate estimate**

429 In the GCB, the global atmospheric CO₂ annual growth rate is derived from CO₂ mole fraction
430 observations at the surface (in ppm/yr) which are converted to mass growth rates (G_{ATM}, in
431 GtC/yr) using a conversion factor (CF) with a constant value of 2.124 GtC/ppm ⁴⁶. Here, we
432 estimate the uncertainty in CF and hence G_{ATM}, using the 14 atmospheric inversions included in
433 GCB2024, following the method by van der Woude et al. ⁵⁷. We use the model-sampled mole
434 fractions at the surface stations to calculate the annual CO₂ growth rate (in ppm/yr), following
435 the same calculation for the observations as developed by ⁴¹, similar to the method used by the
436 National Oceanic and Atmospheric Administration (NOAA) ³⁹. We calculate the annual net input
437 of CO₂ in the atmosphere (in GtC/yr) as the sum of the annual fossil fuel emissions and the
438 inverse-derived net land and ocean sinks. The annual ratio of this net annual input of CO₂
439 divided by the annual growth rate gives the CF (in GtC/ppm). This is repeated for each inverse
440 model and results in annual estimates of the CF (Extended Data Fig. 4a), with their standard
441 deviation. Note that not all inversions are available over the complete period, and we therefore
442 focus the analysis on the period covered by most inversions (2001-2023). CF shows statistically
443 significant interannual variability that is larger than the standard deviation of the 14 inverse
444 models (Extended Data Fig. 4a). We subsequently propagate the uncertainty in CF resulting from
445 1) the annual uncertainty in the observation-based growth rate, 2) the mean interannual
446 variability over the 2001-2023 period and 3) the mean standard deviation of the inversions over
447 2001-2023, to estimate the resulting uncertainty on G_{ATM} (in GtC/yr) (Extended Data Fig. 4b).
448 Finally, we propagate this combined uncertainty to the GCB B_{IM}, where the uncertainty band
449 represents the uncertainty in the B_{IM} explained by the G_{ATM} uncertainty (Extended Data Fig.
450 4c). Years within this uncertainty band therefore do not have a statistically significant B_{IM}. No
451 adjustment on G_{ATM} itself is made here as the year-to-year changes in CF need further
452 evaluation.

453

454 **Climate change impact on the global carbon budget**

455 The land and ocean sinks in the GCB account for both the effect of increasing atmospheric CO₂
456 and climate change over the historical period. As described in GCB2024, the DGVMs and
457 GOBMs performed two simulations: one accounting for changes in atmospheric CO₂ and
458 climate, and one with the same prescribed increase in atmospheric CO₂, but with a constant
459 climate forcing, representative of a natural climate (1900-1910 for the DGVMs, late 1950s for
460 the GOBMs). The difference between these two simulations is the effect of climate change on
461 the land and ocean sinks (S_{LAND}^{clim} , S_{OCEAN}^{clim}), as simulated by the DGVMs and GOBMs (Fig.
462 2, Extended Data Fig. 5). We add these climate change effects on the revised estimates of S_{LAND}
463 and S_{OCEAN} to estimate the land and ocean sinks in the absence of climate change. The impact on
464 atmospheric CO₂ (Fig. 2c) is estimated as $G_{ATM}^{clim} = AF \times (S_{LAND}^{clim} + S_{OCEAN}^{clim})$, where AF is
465 the airborne fraction. The theoretical atmospheric CO₂ growth rate, in the absence of climate
466 change, is then estimated as $G_{ATM} - G_{ATM}^{clim}$.
467

468 Additional references

469

470 47. Gasser, T. *et al.* The compact Earth system model OSCAR v2.2: description and first
471 results. *Geosci. Model Dev.* **10**, 271–319 (2017).

472 48. O’Sullivan, M. *et al.* An improved approach to estimate the natural land carbon sink. Preprint
473 at <https://doi.org/10.21203/rs.3.rs-7207206/v1> (2025).

474 49. Liu, M. *et al.* Global riverine land-to-ocean carbon export constrained by observations and
475 multi-model assessment. *Nat. Geosci.* **17**, 896–904 (2024).

476 50. Terhaar, J., Frölicher, T. L. & Joos, F. Observation-constrained estimates of the global
477 ocean carbon sink from Earth system models. *Biogeosciences* **19**, 4431–4457 (2022).

478 51. Goris, N. *et al.* Constraining projection-based estimates of the future North Atlantic carbon
479 uptake. <https://doi.org/10.1175/JCLI-D-17-0564.1> (2018) doi:10.1175/JCLI-D-17-0564.1.

480 52. Terhaar, J., Frölicher, T. L. & Joos, F. Southern Ocean anthropogenic carbon sink
481 constrained by sea surface salinity. *Sci. Adv.* **7**, eabd5964 (2021).

482 53. Bourgeois, T., Goris, N., Schwinger, J. & Tjiputra, J. F. Stratification constrains future heat
483 and carbon uptake in the Southern Ocean between 30°S and 55°S. *Nat. Commun.* **13**, 340
484 (2022).

485 54. Dong, Y. *et al.* Direct observational evidence of strong CO₂ uptake in the Southern Ocean.
486 *Sci. Adv.* **10**, eadn5781 (2024).

487 55. Bellenger, H. *et al.* Sensitivity of the global ocean carbon sink to the ocean skin in a climate
488 model. *J. Geophys. Res. Oceans* **128**, e2022JC019479 (2023).

489 56. Woolf, D. K., Land, P. E., Shutler, J. D., Goddijn-Murphy, L. M. & Donlon, C. J. On the
490 calculation of air-sea fluxes of CO₂ in the presence of temperature and salinity gradients. *J.*
491 *Geophys. Res. Oceans* **121**, 1229–1248 (2016).

492 57. van der Woude, A. *et al.* A top-down view of global and regional carbon budgets from an
493 ensemble of atmospheric inversions.
494 <https://www.authorea.com/doi/full/10.22541/essoar.175376114.45413910/v1?commit=dd606630ddad79961983787e20e0384e5b2c5b32>.
496

497 Acknowledgements

498 We thank the Global Carbon Project, Rob Jackson, and all contributors to annual updates of the
499 global carbon budget, which have informed continuous assessments of our understanding of the
500 carbon cycle and its evolution under human pressure. This work received support through
501 Schmidt Sciences, LLC (VESRI CALIPSO project and OBI InMOS project). CLQ was
502 supported by the UK Royal Society (RSRP\R\241002). MWJ was funded by the Natural
503 Environment Research Council (NE/V01417X/1). GPP and RMA were supported by the
504 Research Council of Norway (NorSink, 352474). AvdW, WP and ITL received funding from the
505 Netherlands Organisation for Scientific Research (grant no. NWO-2023.003 and
506 VI.Vidi.213.143). HT acknowledges support from US Department of Agriculture (TENX12899).
507 JGC was supported by Australia's NESP2-Climate Systems Hub. JH acknowledges funding from
508 ERC-2022-STG OceanPeak (grant no. 101077209) (European Commission). The work reflects
509 only the authors' view; the European Commission and their executive agency are not responsible
510 for any use that may be made. For the purpose of open access, the author has applied a Creative
511 Commons Attribution (CC BY) licence to any Author Accepted Manuscript version arising from
512 this submission.

513

514 Author contributions

515 PF and CLQ designed the study and drafted the manuscript. JP, CS and TG provided the revised
516 land-use emission estimate, MOS, SS, PR, and HT provided the revised land sink estimate, JH,
517 PL, DCEB, AO and CLQ provided the revised ocean sink estimate. ITL, WP, AvdW, XL, EM
518 and HL assessed the variability and uncertainty in the atmospheric concentration growth rate.
519 RMA and GPP assessed the fossil emissions estimate. MWJ, JGC, PC commented on the draft.
520 All authors contributed to the writing of the manuscript.

521

522 Supplementary Information is available for this paper.

523 Correspondence and requests for materials should be addressed to P. Friedlingstein
524 (p.friedlingstein@exeter.ac.uk).

525 Reprints and permissions information is available at www.nature.com/reprints.

526

527 Data availability

528 All data presented in this manuscript are available on Zenodo

529 (<https://zenodo.org/records/16367993>).

530 Code availability

531 No new code was generated for this study. Figures with maps were done using the R statistical

532 environment.

533

534 The authors declare no competing interests

535 References

536

537

538 1. Friedlingstein, P. *et al.* Global Carbon Budget 2024. *Earth Syst. Sci. Data* **17**, 965–1039

539 (2025).

540 2. Forster, P. M. *et al.* Indicators of Global Climate Change 2024: annual update of key
541 indicators of the state of the climate system and human influence. *Earth Syst. Sci. Data* **17**,
542 2641–2680 (2025).

543 3. Keeling, R. F. & Manning, A. C. Studies of recent changes in atmospheric O₂ content. in
544 *Treatise on Geochemistry* (eds H. Holland & K. Turekian) vol. 5.15 385–404 (Elsevier,
545 Amsterdam, 2014).

546 4. Gruber, N. *et al.* The oceanic sink for anthropogenic CO₂ from 1994 to 2007. *Science* **363**,
547 1193–1199 (2019).

548 5. Keeling, C. D. The concentration and isotopic abundances of carbon dioxide in the
549 atmosphere. *Tellus* **12B**, 200–203 (1960).

550 6. Bolin, B. & Bischof, W. Variations of the carbon dioxide content of the atmosphere in the
551 northern hemisphere. *Tellus* **22**, 431–442 (1970).

552 7. Tans, P. P., Fung, I. Y. & Takahashi, T. Observational constraints on the global atmospheric
553 CO₂ budget. *Science* **247**, 1431–1438 (1990).

554 8. Norby, R. J. *et al.* Forest response to elevated CO₂ is conserved across a broad range of
555 productivity. *Proc. Natl. Acad. Sci. U. S. A.* **102**, 18052–18056 (2005).

556 9. Pan, Y. D. *et al.* A large and persistent carbon sink in the world's forests. *Science* **333**, 988–
557 993 (2011).

558 10. Cramer, W. *et al.* Global response of terrestrial ecosystem structure and function to CO₂ and
559 climate change: results from six dynamic global vegetation models. *Glob. Change Biol.* **7**,
560 357–373 (2001).

561 11. Canadell, J. G. *et al.* Contributions to accelerating atmospheric CO₂ growth from economic
562 activity, carbon intensity, and efficiency of natural sinks. *Proc. Natl. Acad. Sci. U. S. A.* **104**,
563 18,866–18,870 (2007).

564 12. Canadell, J. G. Global Carbon and Other Biogeochemical Cycles and Feedbacks. in *Climate
565 Change 2021 – The Physical Science Basis: Working Group I Contribution to the Sixth
566 Assessment Report of the Intergovernmental Panel on Climate Change* (Cambridge
567 University Press, Cambridge, 2021).

568 13. Houghton, R. A. *et al.* Changes in the carbon content of terrestrial biota and soils between
569 1860 and 1980: A net release of CO₂ to the atmosphere. *Ecol. Monogr.* **53**, 236–262 (1983).

570 14. Houghton, R. A. *et al.* Carbon emissions from land use and land-cover change.
571 *Biogeosciences* **9**, 5125–5142 (2012).

572 15. Pongratz, J., Reick, C. H., Houghton, R. A. & House, J. I. Terminology as a key uncertainty
573 in net land use and land cover change carbon flux estimates. *Earth Syst. Dyn.* **5**, 177–195
574 (2014).

575 16. Walker, A. P. *et al.* Harmonizing direct and indirect anthropogenic land carbon fluxes
576 indicates a substantial missing sink in the global carbon budget since the early 20th century.
577 *Plants People Planet* **7**, 1123–1136 (2025).

578 17. Dorgeist, L., Schwingshackl, C., Bultan, S. & Pongratz, J. A consistent budgeting of
579 terrestrial carbon fluxes. *Nat. Commun.* **15**, 7426 (2024).

580 18. Gasser, T. *et al.* Historical CO₂ emissions from land use and land cover change and their
581 uncertainty. *Biogeosciences* **17**, 4075–4101 (2020).

582 19. Strassmann, K. M., Joos, F. & Fischer, G. Simulating effects of land use changes on carbon
583 fluxes: Past contributions to atmospheric CO₂ increases and future commitments due to
584 losses of terrestrial sink capacity. *Tellus Ser. B-Chem. Phys. Meteorol.* **60**, 583–603 (2008).

585 20. Obermeier, W. A. *et al.* Modelled land use and land cover change emissions – a spatio-
586 temporal comparison of different approaches. *Earth Syst. Dyn.* **12**, 635–670 (2021).

587 21. Gasser, T. & Ciais, P. A theoretical framework for the net land-to-atmosphere CO₂ flux and
588 its implications in the definition of 'emissions from land-use change'. *Earth Syst. Dyn.* **4**,
589 171–186 (2013).

590 22. Regnier, P. *et al.* Anthropogenic perturbation of the carbon fluxes from land to ocean. *Nat.*
591 *Geosci.* **6**, 597–607 (2013).

592 23. Lacroix, F., Ilyina, T. & Hartmann, J. Oceanic CO₂ outgassing and biological production
593 hotspots induced by pre-industrial river loads of nutrients and carbon in a global modeling
594 approach. *Biogeosciences* **17**, 55–88 (2020).

595 24. Regnier, P., Resplandy, L., Najjar, R. G. & Ciais, P. The land-to-ocean loops of the global
596 carbon cycle. *Nature* **603**, 401–410 (2022).

597 25. Tian, H. *et al.* Increased Terrestrial carbon export and CO₂ evasion from global inland
598 waters since the preindustrial era. *Glob. Biogeochem. Cycles* **37**, e2023GB007776 (2023).

599 26. Bakker, D. C. E. *et al.* A multi-decade record of high-quality fCO₂ data in version 3 of the
600 Surface Ocean CO₂ Atlas (SOCAT). *Earth Syst. Sci. Data* **8**, 383–413 (2016).

601 27. Rödenbeck, C. *et al.* Data-based estimates of the ocean carbon sink variability – first results
602 of the Surface Ocean pCO₂ Mapping intercomparison (SOCOM). *Biogeosciences* **12**, 7251–
603 7278 (2015).

604 28. Mayot, N. *et al.* Constraining the trend in the ocean CO₂ sink during 2000–2022. *Nat.*
605 *Commun.* **15**, 8429 (2024).

606 29. Hauck, J. *et al.* The Southern Ocean carbon cycle 1985–2018: mean, seasonal cycle,
607 trends, and storage. *Glob. Biogeochem. Cycles* **37**, e2023GB007848 (2023).

608 30. Behncke, J., Landschützer, P. & Tanhua, T. A detectable change in the air-sea CO₂ flux
609 estimate from sailboat measurements. *Sci. Rep.* **14**, 3345 (2024).

610 31. Mayot, N. *et al.* Climate-driven variability of the Southern Ocean CO₂ sink. *Philos. Trans. R.*
611 *Soc. Math. Phys. Eng. Sci.* **381**, 20220055 (2023).

612 32. Terhaar, J. *et al.* Assessment of global ocean biogeochemistry models for ocean carbon
613 sink estimates in RECCAP2 and recommendations for future studies. *J. Adv. Model. Earth
614 Syst.* **16**, e2023MS003840 (2024).

615 33. Müller, J. D. *et al.* Decadal trends in the oceanic storage of anthropogenic carbon from 1994
616 to 2014. *AGU Adv.* **4**, e2023AV000875 (2023).

617 34. Terhaar, J. Composite model-based estimate of the ocean carbon sink from 1959 to 2022.
618 *Biogeosciences* **22**, 1631–1649 (2025).

619 35. Watson, A. J. *et al.* Revised estimates of ocean-atmosphere CO₂ flux are consistent with
620 ocean carbon inventory. *Nat. Commun.* **11**, 4422 (2020).

621 36. Dong, Y. *et al.* Update on the temperature corrections of global air-sea CO₂ flux estimates.
622 *Glob. Biogeochem. Cycles* **36**, e2022GB007360 (2022).

623 37. Ford, D. J. *et al.* Enhanced ocean CO₂ uptake due to near-surface temperature gradients.
624 *Nat. Geosci.* **17**, 1135–1140 (2024).

625 38. Andrew, R. M. A comparison of estimates of global carbon dioxide emissions from fossil
626 carbon sources. *Earth Syst. Sci. Data* **12**, 1437–1465 (2020).

627 39. Lan, X., Tans, P., & Thoning K.W. Trends in CO₂ - NOAA Global Monitoring Laboratory.
628 <https://gml.noaa.gov/ccgg/trends/global.html>.

629 40. Ballantyne, A. P., Alden, C. B., Miller, J. B., Tans, P. P. & White, J. W. C. Increase in
630 observed net carbon dioxide uptake by land and oceans during the last 50 years. *Nature*
631 **488**, 70–72 (2012).

632 41. Wu, Z. *et al.* Investigating the differences in calculating global mean surface CO₂
633 abundance: the impact of analysis methodologies and site selection. *Atmospheric Chem.
634 Phys.* **24**, 1249–1264 (2024).

635 42. Tohjima, Y., Mukai, H., Machida, T., Hoshina, Y. & Nakaoka, S.-I. Global carbon budgets
636 estimated from atmospheric O₂N₂ and CO₂ observations in the western Pacific region over
637 a 15-year period. *Atmospheric Chem. Phys.* **19**, 9269–9285 (2019).

638 43. Arora, V. K. *et al.* Carbon–concentration and carbon–climate feedbacks in CMIP6 models
639 and their comparison to CMIP5 models. *Biogeosciences* **17**, 4173–4222 (2020).

640 44. Bansen, F., Nissen, C. & Hauck, J. The impact of recent climate change on the global ocean
641 carbon sink. *Geophys. Res. Lett.* **51**, e2023GL107030 (2024).

642 45. Gatti, L. V. *et al.* Amazonia as a carbon source linked to deforestation and climate change.
643 *Nature* **595**, 388–393 (2021).

644 46. Hubau, W. *et al.* Asynchronous carbon sink saturation in African and Amazonian tropical
645 forests. *Nature* **579**, 80–87 (2020).

646

647

648 Figures legend

649 **Figure 1. Revised components of the global carbon budget.** Top left panel: net land-use
650 emissions (ELUC). Top right panel: land sink (SLAND). Bottom left panel: ocean sink (SOCEAN).
651 Bottom right panel: budget imbalance (BIM). Grey bars on the left show the GCB2024 estimate,
652 intermediate bars show the incremental corrections from this study, and colour bars on the right
653 show the consolidated estimates. Units are GtC/yr. Components are averaged over the last
654 decade (2014-2023). δL , RSS and LCE respectively refer to the transient carbon densities
655 correction, the replaced sinks and sources correction, and the lateral carbon export correction, see
656 Methods.

657

658 **Figure 2. Impact of climate change on carbon sinks and atmospheric CO₂ increase** Impact
659 of climate change on (a) the ocean sink (SOCEAN) as simulated by GOBMs (GtC/yr), (b) the land
660 sink (SLAND) as simulated by DGVMs (GtC/yr), and (c) their cumulative effect on the
661 atmospheric CO₂ concentration increase since 1960 (ppm).

662

663 **Figure 3. Consolidated global carbon budget.** Fossil CO₂ emissions (EfOS), the revised net
664 land-use change emissions (ELUC), the revised land sink and ocean sink (SLAND and SOCEAN) both
665 separated into their response to CO₂ and response to climate, the atmospheric CO₂ growth rate
666 (GATM) and the residual budget imbalance (BIM). Units are GtC/yr. Components are averaged
667 over the last decade (2014-2023). Dashed outlines indicate a new update in this study compared
668 to GCB2024.

669

670 **Figure 4. Land CO₂ fluxes and attribution effects.** Decadal mean (2014-2023) of the net land
671 CO₂ flux (SLAND-ELUC) (central map and grey bars for each land RECCAP region) and attribution
672 to the effects of atmospheric CO₂ increase (CO₂ fertilization; green bars), climate impact (red
673 bars), and land-use change (orange bars). Units are gC/m²/yr for the spatial map and MtC/yr for
674 the integrals over the RECCAP regions. CO₂ and climate flux uncertainties calculated as the 1
675 sigma spread among DGVMs from GCB2024. ELUC uncertainty is calculated as the 1 sigma
676 spread among Bookkeeping models from GCB2024. The uncertainty on the net flux is the square
677 root of the sum of squares of the three component fluxes.

678

679 Table 1. Global carbon budget as in GCB2024 and consolidated budget from this study. Annual
 680 CO₂ fluxes averaged over the 2014-2023 decade. Units are GtC/yr.
 681

	G_{ATM}	E_{FOS}	E_{LUC}	S_{LAND}	Net Land	S_{OCEAN}	B_{IM}
GCB2024	5.2±0.02	9.7±0.5	1.1±0.7	3.2±0.9	2.1±1.1	2.9±0.4	-0.4±1.3
This study	5.2±0.02	9.7±0.5	1.2±0.7	2.7±0.9	1.4±1.1	3.1±0.5	-0.02±1.3
<i>Difference</i>	<i>0</i>	<i>0</i>	<i>+0.1</i>	<i>-0.5</i>	<i>-0.6</i>	<i>+0.2</i>	<i>+0.4</i>
Atmospheric inversions	5.2±0.0	9.7±0.5	N/A	N/A	1.4±0.5	3.1±0.5	0
Atmospheric oxygen	5.2±0.0	9.7±0.5	N/A	N/A	1.0±0.8	3.4±0.5	0

682
 683 * Net land is the net land CO₂ flux, calculated as S_{LAND} - E_{LUC}. Atmospheric inversions and
 684 atmospheric oxygen do provide Net Land but do not separate E_{LUC} from S_{LAND}. The budget
 685 imbalance (B_{IM}) is the difference between anthropogenic net emissions (E_{FOS}+E_{LUC}) and
 686 accumulation of carbon in the atmosphere, land and ocean (G_{ATM}+S_{LAND}+S_{OCEAN}). By design,
 687 atmospheric inversions and atmospheric oxygen budget imbalance is null. The uncertainty
 688 represents ± 1 standard deviation as in ref. ¹.
 689

690 Extended Data Figures legend

691 **Extended Data Figure 1 | Budget imbalance** (B_{IM}) as reported in the GCB2024, as reported in the GCB2024, showing a statistically significant
692 negative trend (dotted line) of -0.14 ± 0.04 GtC/yr per decade ($p\text{-value}=0.003$). Units are GtC/yr.

693
694 **Extended Data Figure 2 | Consolidated global carbon budget.** Revision (in red) compared to the GCB2024 estimate (in black) of (b) net land-use
695 emissions, (c) ocean sink, (d) land sink, and (f) budget imbalance. Panels (a) fossil CO₂ emissions and (e) atmospheric CO₂ growth rate are
696 unchanged. All fluxes are in GtC/yr.

697
698 **Extended Data Figure 3 | Impact of lateral carbon flux correction on SLAND** Global carbon budget (2014-2023) without (a) and with (b) historical
699 changes in lateral carbon fluxes. Units are GtC/yr. The additional green/blue box represents inland waters, and the surrounding green open rectangle
700 represents the whole land system (terrestrial ecosystems and inland waters combined). The perturbations on inland water fluxes follow the
701 nomenclature of ref.²⁴ and represent land-to-inland water flux (F'_{LI}), aquatic CO₂ outgassing (F'_{IA}), aquatic carbon storage (F'_{IS}) and lateral carbon
702 exports to ocean (F'_{IE}). All fluxes were quantified as the mean of values reported by refs.^{24,25} and Zhang, pers. com. F'_{IA} is subdivided into contributions
703 from soil-derived CO₂ (in orange) and CO₂ from soil organic carbon (in red) respired in inland waters. The Δ represents changes in carbon storage in
704 the different reservoirs. The net effect on S_{LAND} is a decrease of 0.07 ± 0.06 GtC/yr. See methods for further details.

705
706 **Extended Data Figure 4 | Atmospheric growth rate.** Annual conversion factors (CF, in GtC/ppm) for converting the observation-based atmospheric
707 growth rate [ppm/yr] to atmospheric mass growth rates [GtC/yr] derived from the 14 atmospheric inversions included in GCB2024 (orange) in
708 comparison to the fixed value currently used in GCB2024 (blue), open symbols represent years in which less than 4 atmospheric inversions are
709 available; (b) atmospheric growth rate (G_{ATM}) with propagated uncertainty from: 1) uncertainty in the annual observation-based growth rate [ppm/yr],
710 shown in blue shading, 2) mean interannual variability in the CF over 2001-2023, and 3) mean standard deviation of the inverse CFs over 2001-
711 2023 (total combined uncertainty shown in orange shading); and (c) the GCB2024 budget imbalance (B_{IM}) [GtC/yr] with the propagated uncertainty in
 G_{ATM} (orange shading).

712
713 **Extended Data Figure 5 | Land CO₂ fluxes.** (a) Land carbon sink due to atmospheric CO₂ increase (CO₂ fertilization) only, (b) effect of climate
714 change on the land carbon flux, (c) land carbon flux due to land-use change, (d) net land CO₂ flux (a+b+c). Positive values indicate sinks, negative
values indicate sources. Units are gC/m²/yr.

715

716

717 Extended Data Tables Title and legend

718

719 Extended Data Table 1

720

721 Title:

722 **Extended Data Table 1 | Decadal average of all components of the consolidated global carbon budget (GtC/yr)**

723

724 *Legend:*

725 *Net Land* is the net land CO₂ flux, calculated as S_{LAND} - E_{LUC}. Atmospheric inversions and atmospheric oxygen do provide *Net Land* but do not separate
726 E_{LUC} from S_{LAND}. The budget imbalance (B_{IM}) is the difference between anthropogenic net emissions (E_{FOS}+E_{LUC}) and accumulation of carbon in the
727 atmosphere, land and ocean (G_{ATM}+S_{LAND}+S_{OCEAN}). By design, atmospheric inversions and atmospheric oxygen budget imbalance is null.

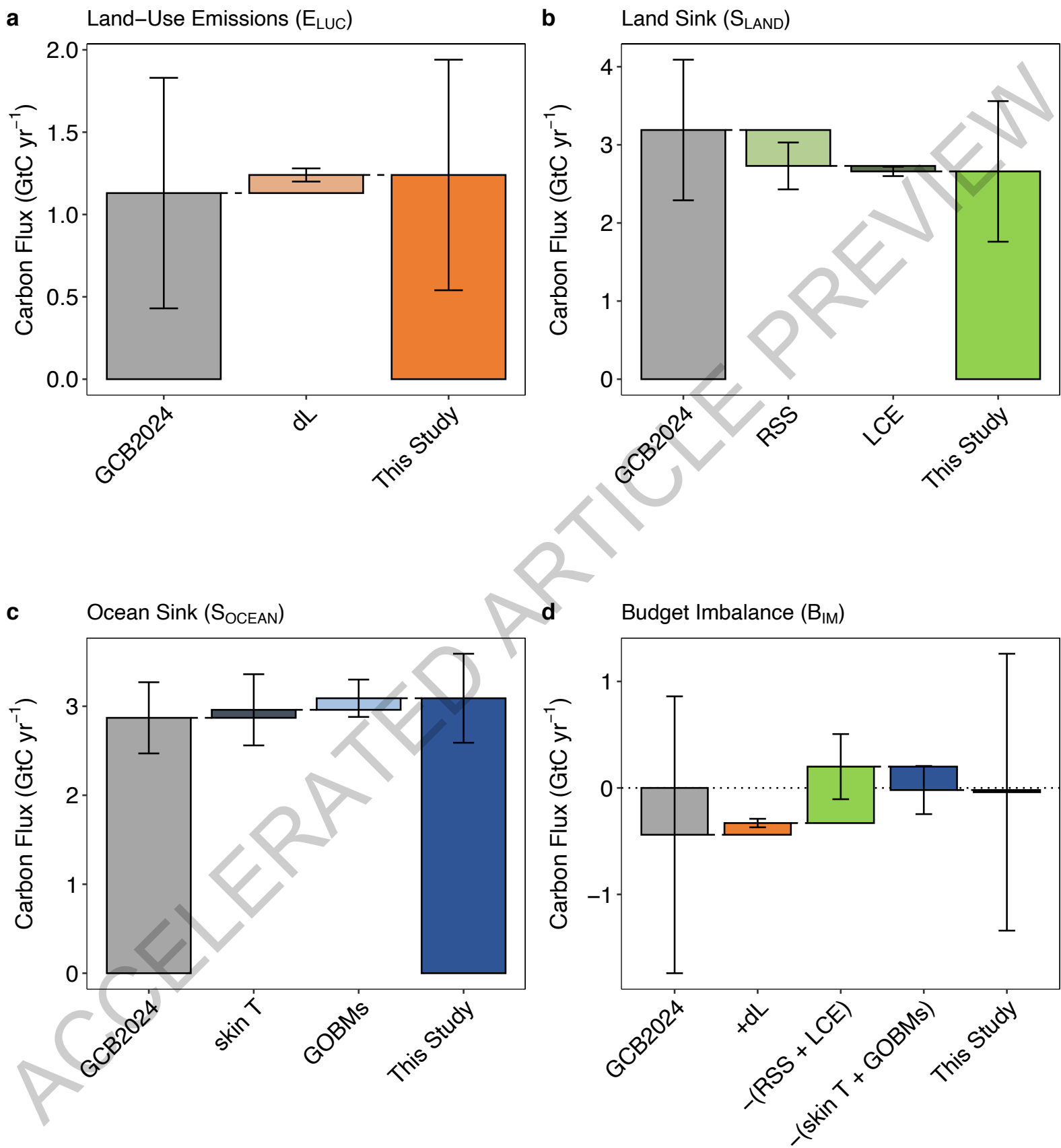
728

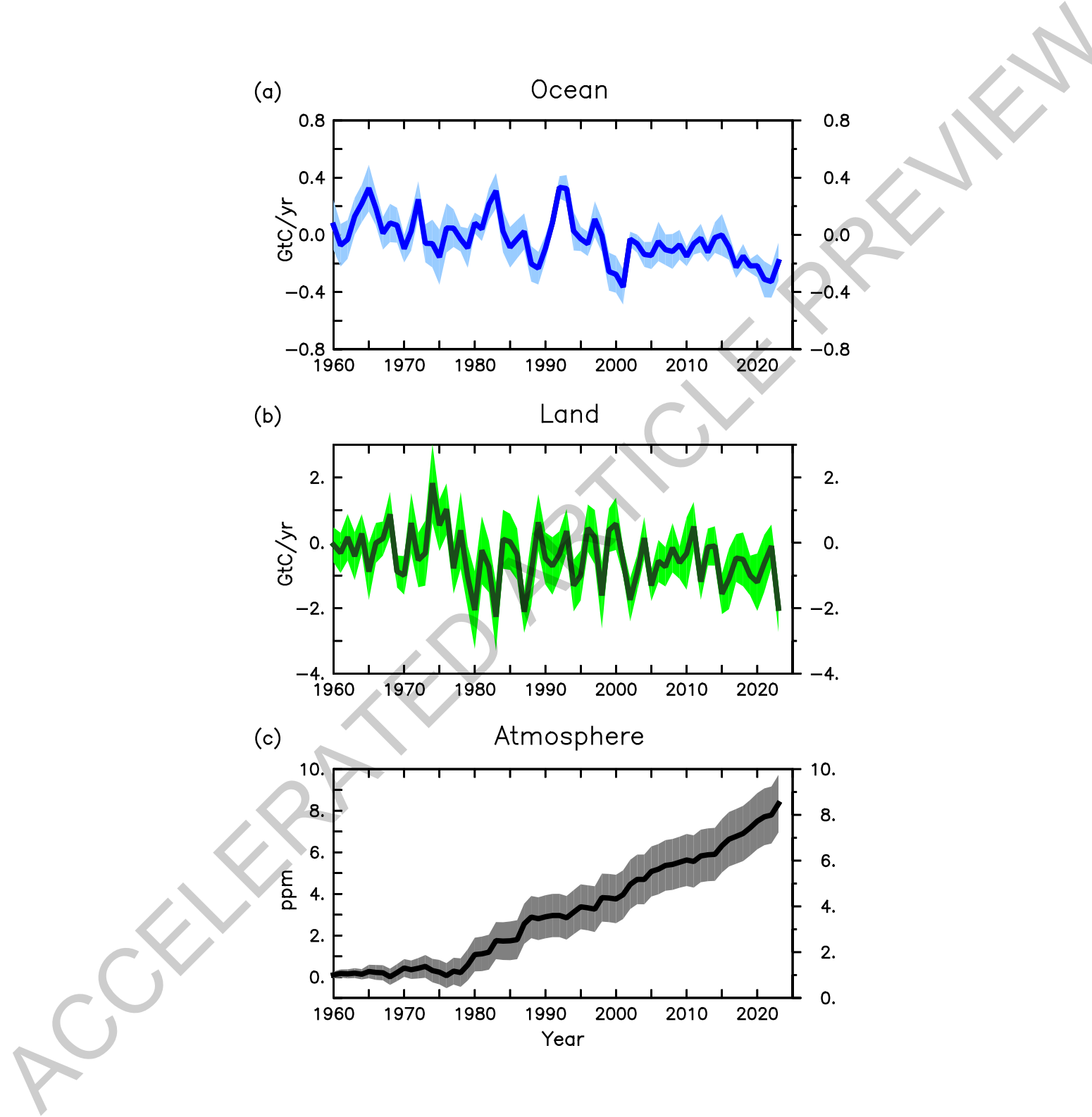
729 Extended Data Table 2

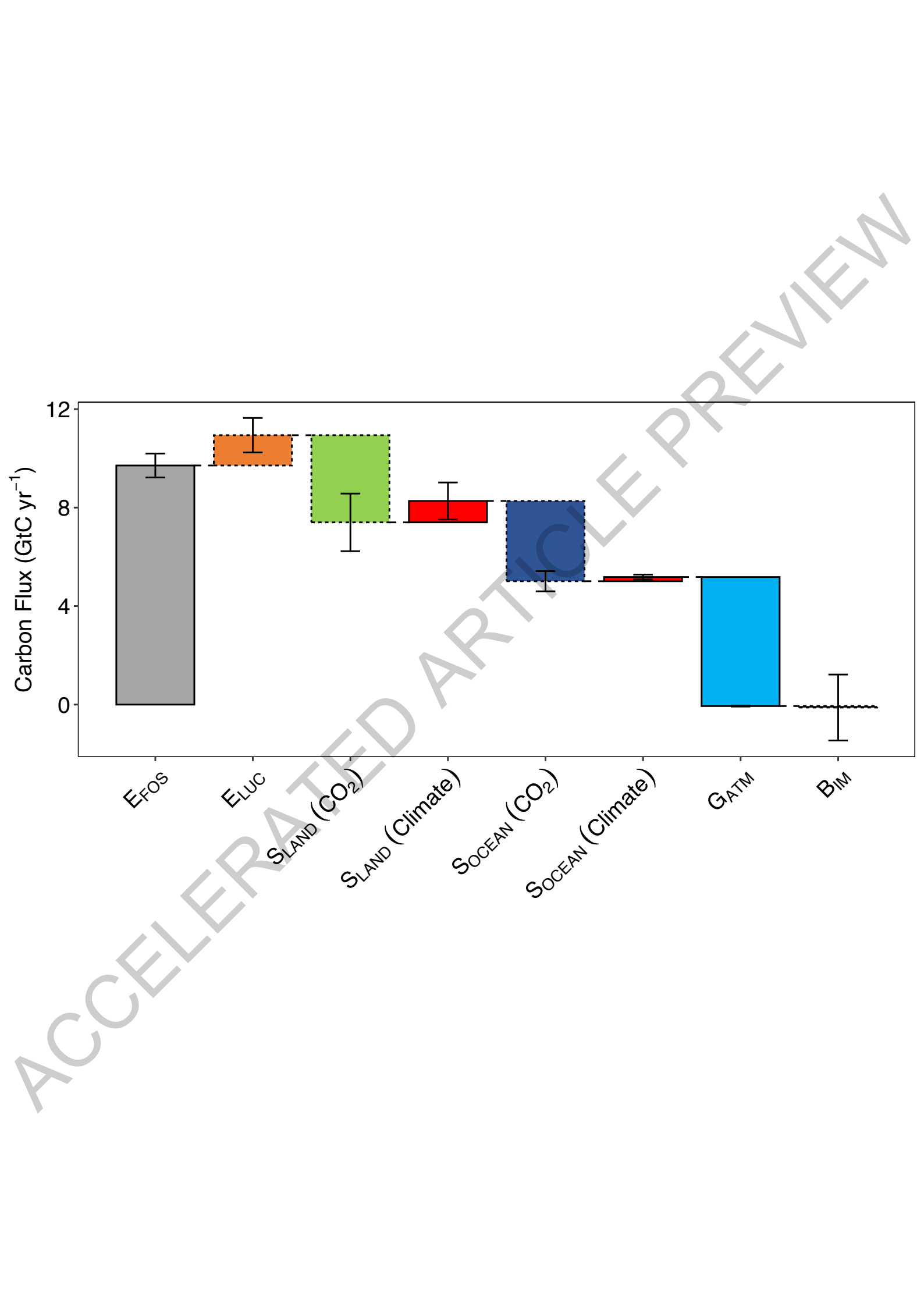
730

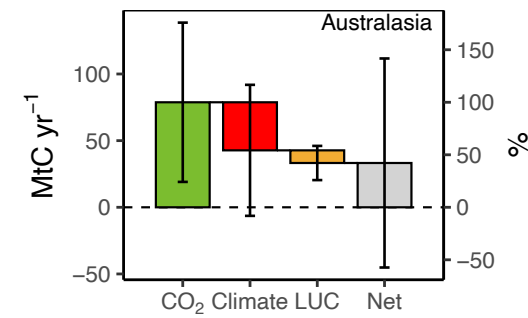
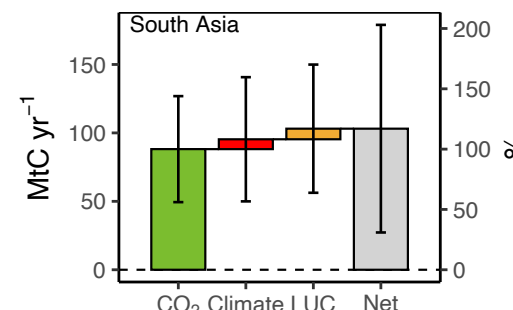
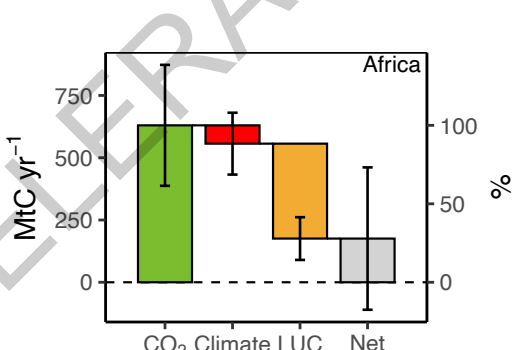
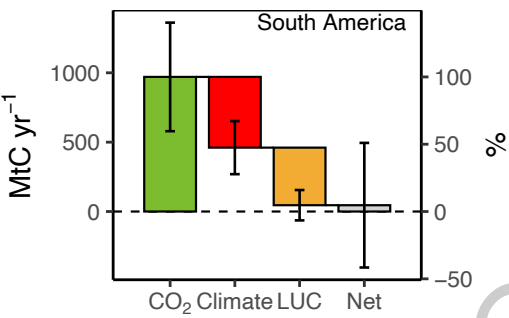
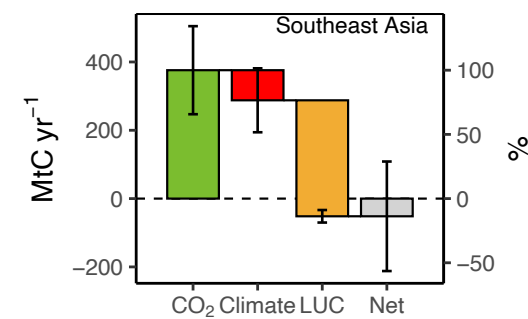
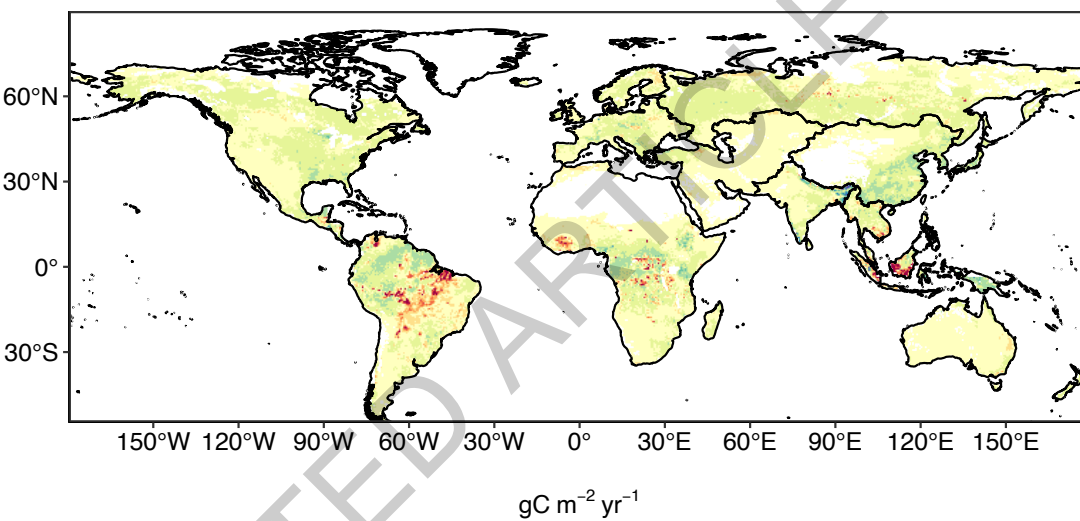
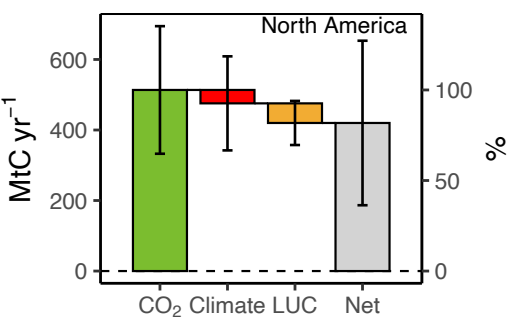
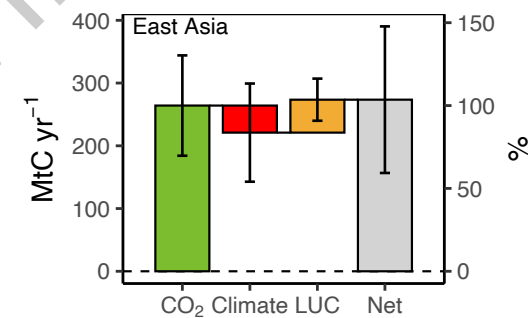
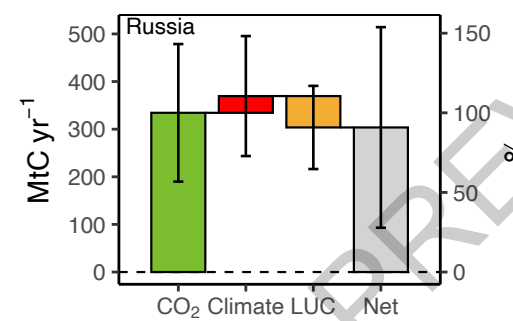
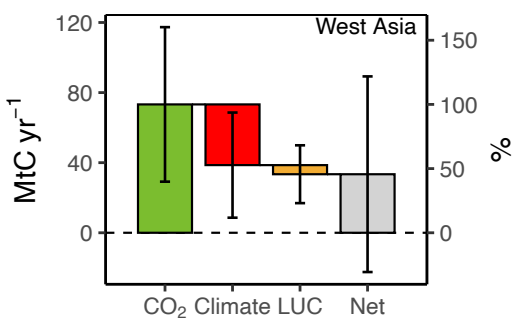
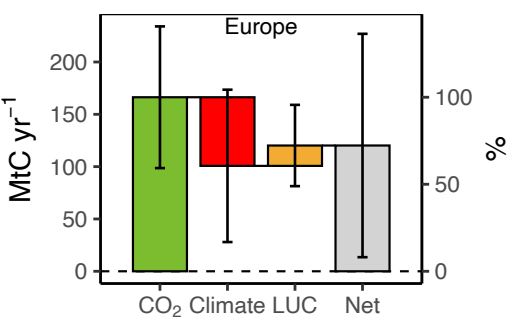
731 Title:

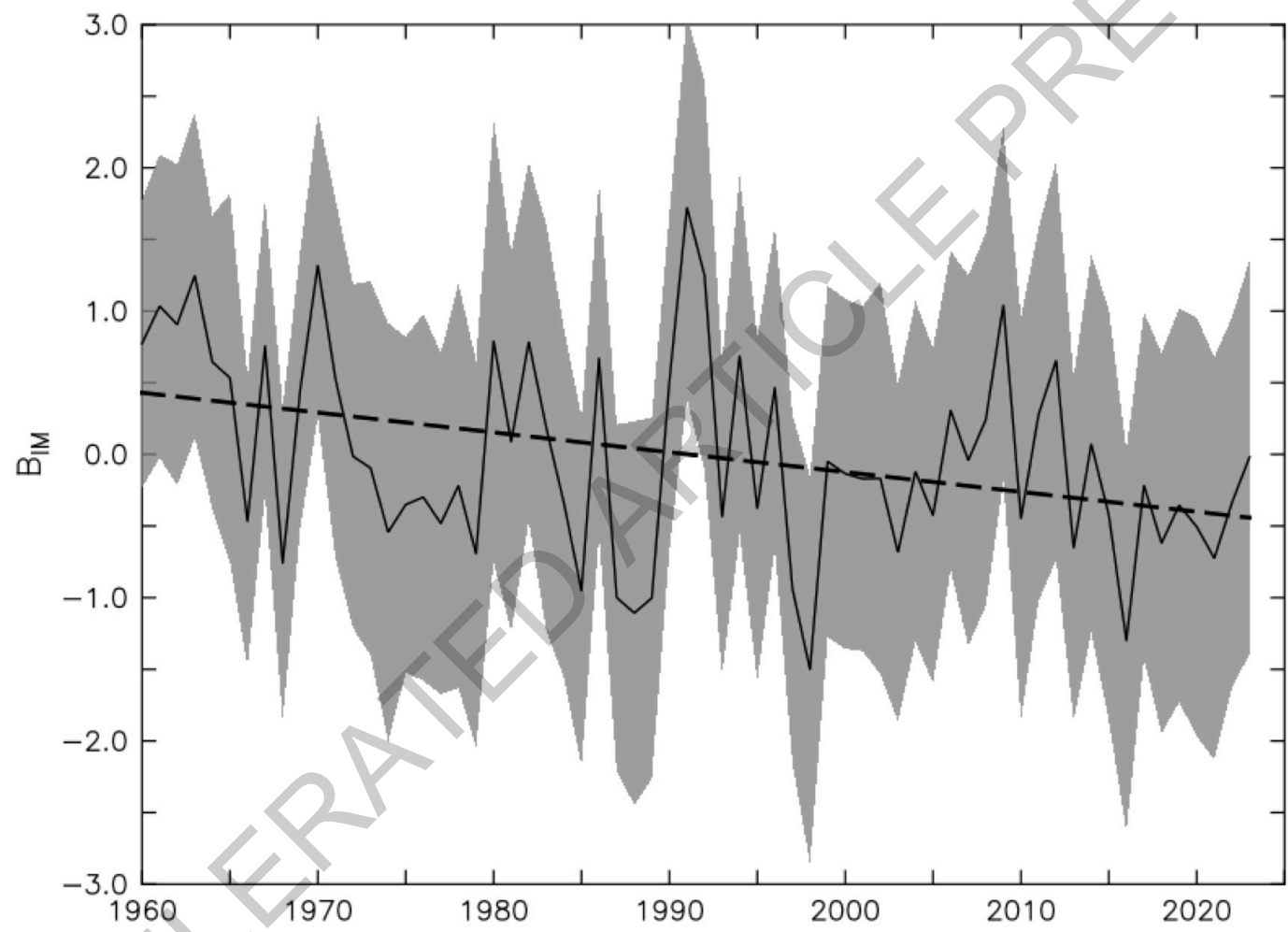
732 **Extended Data Table 2 | Decadal average of all components of the consolidated global carbon budget (GtC/yr)**



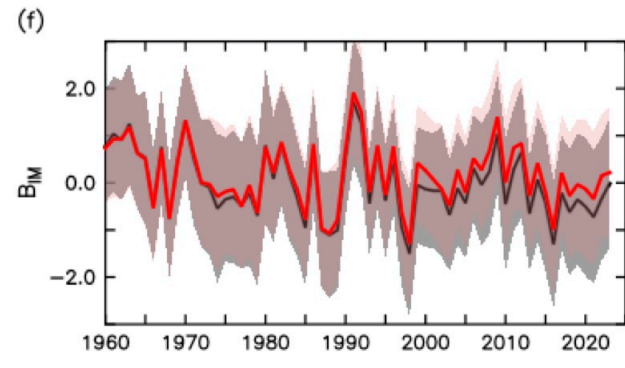
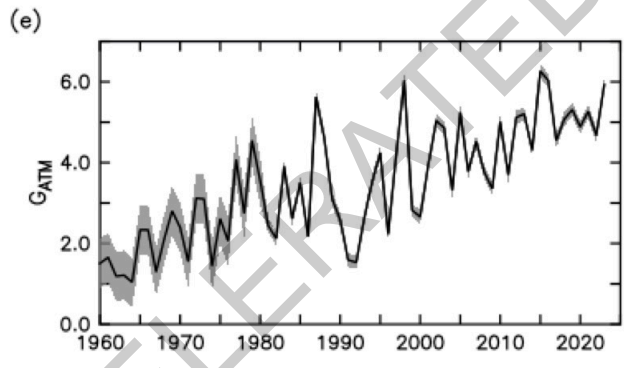
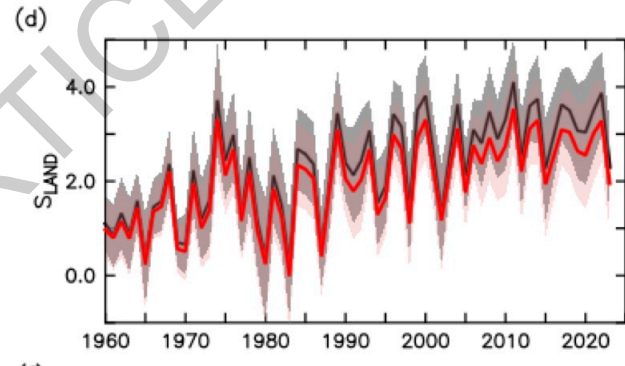
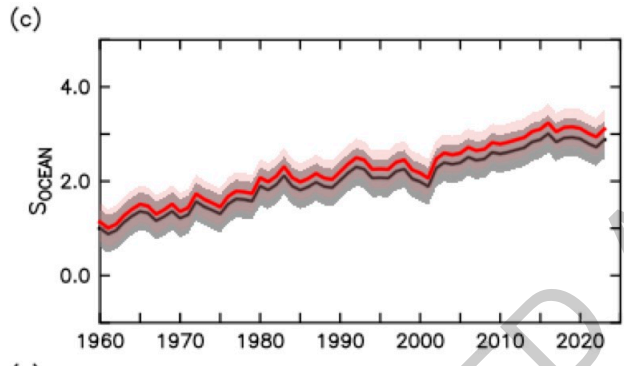
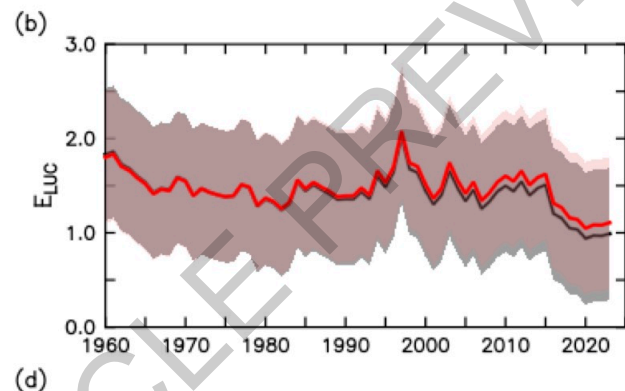
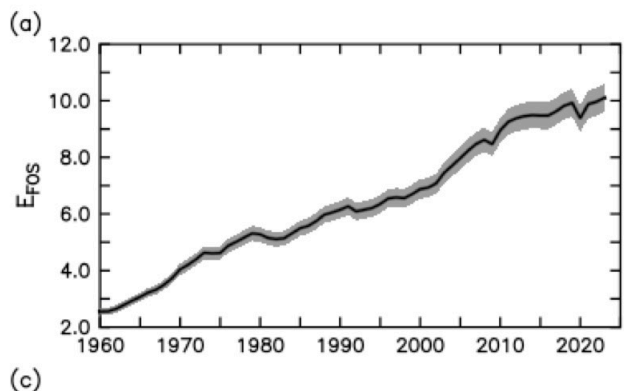




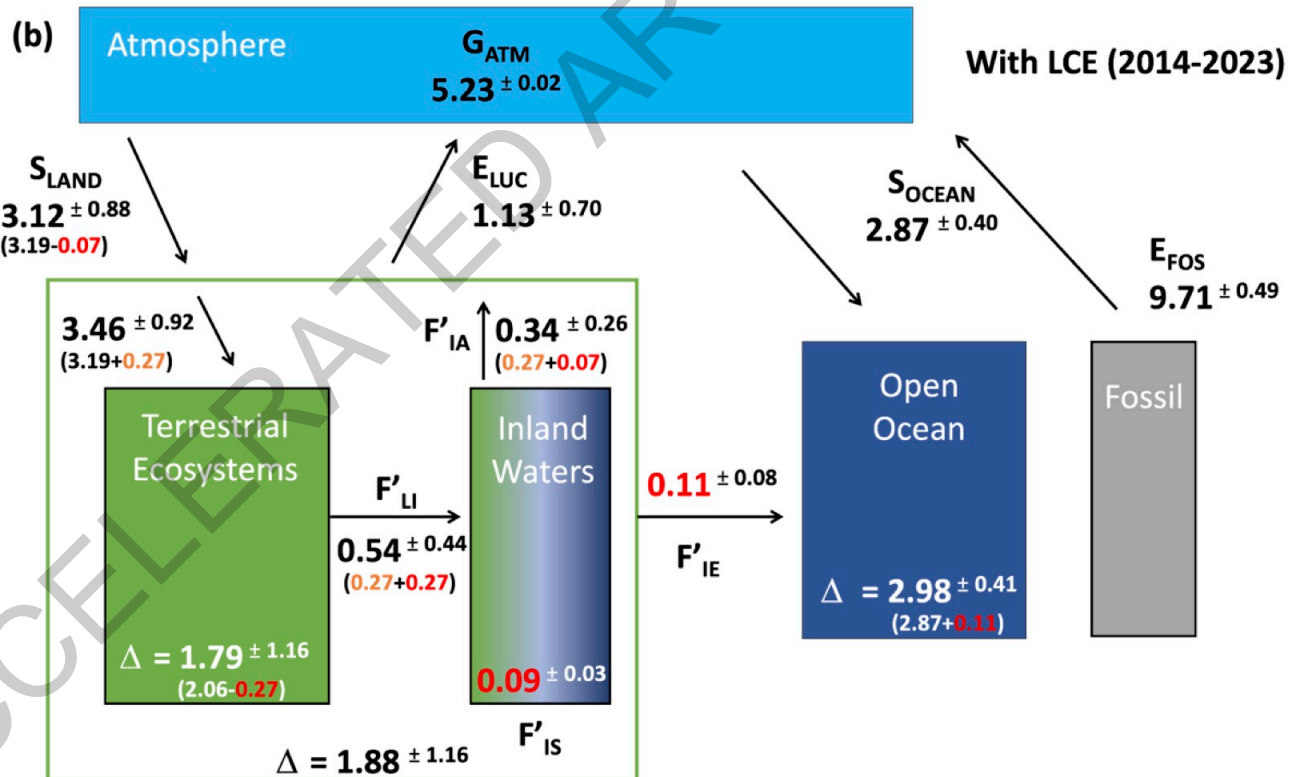
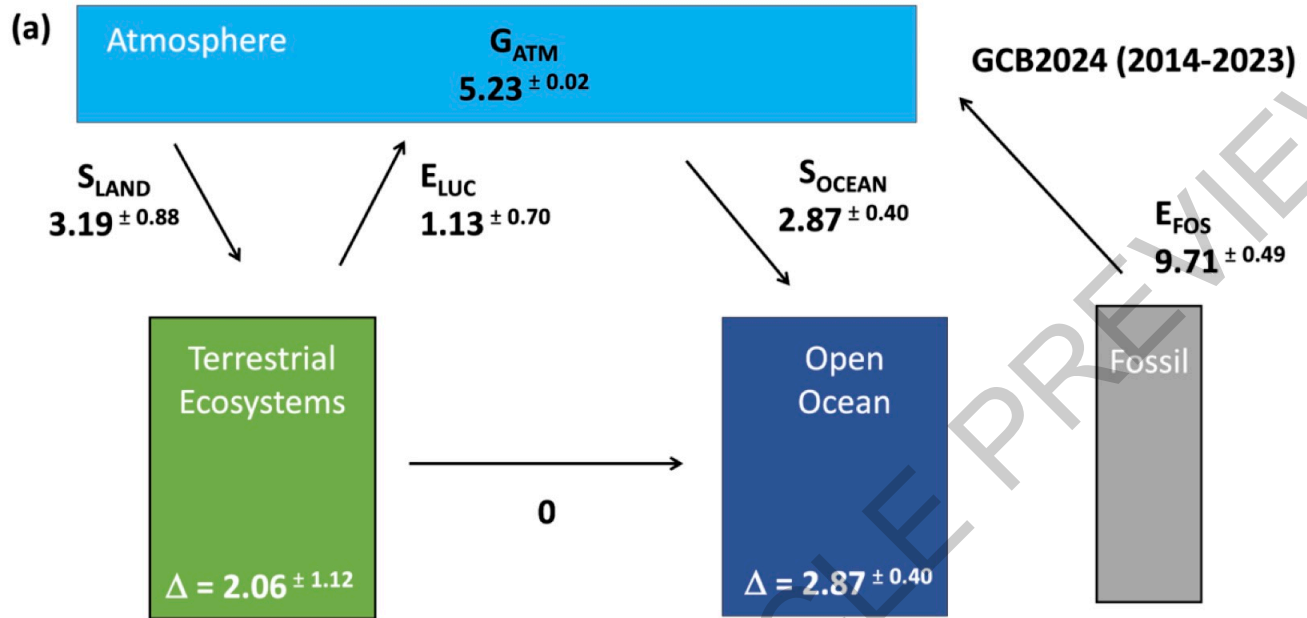




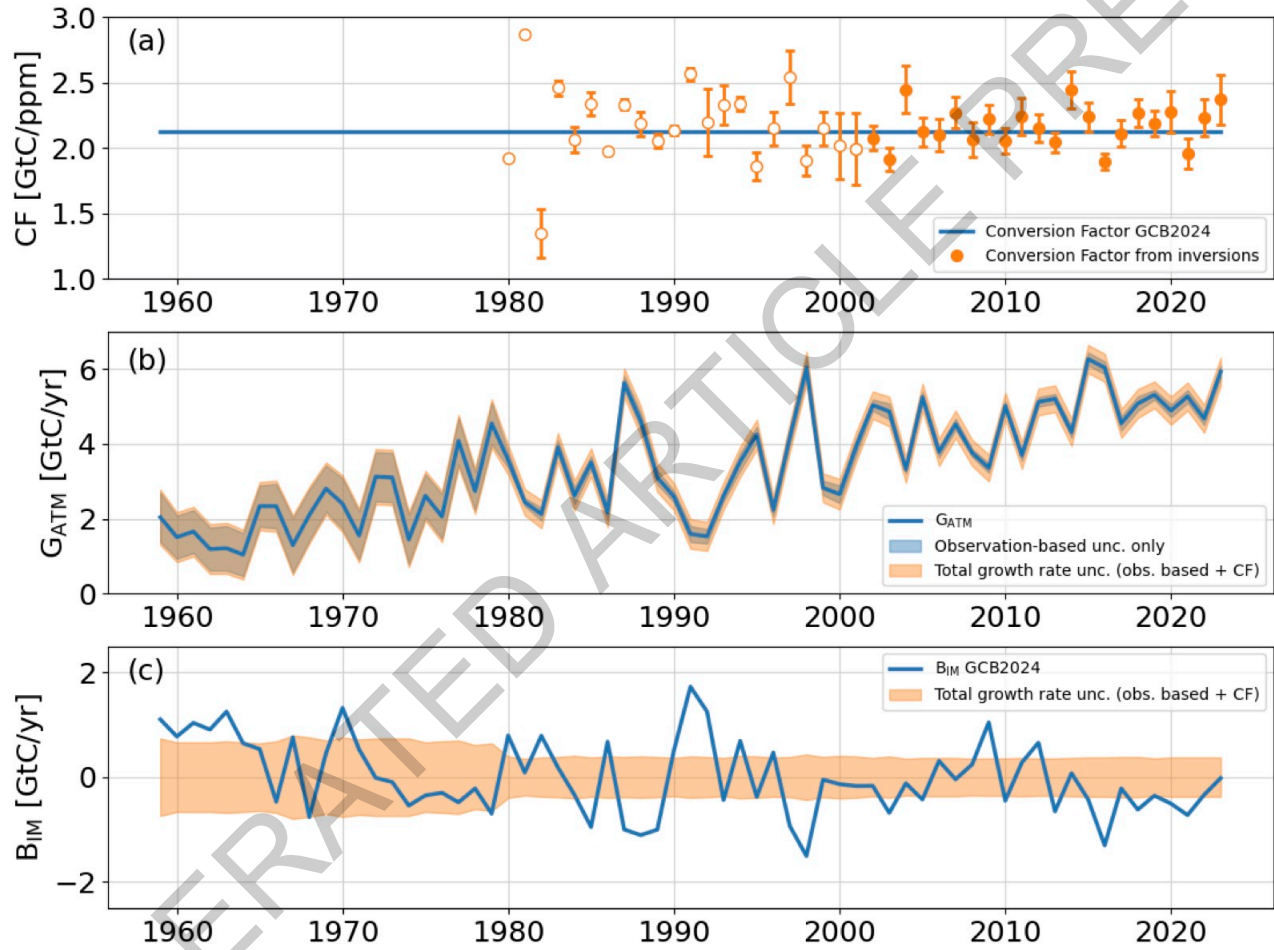
Extended Data Fig. 1



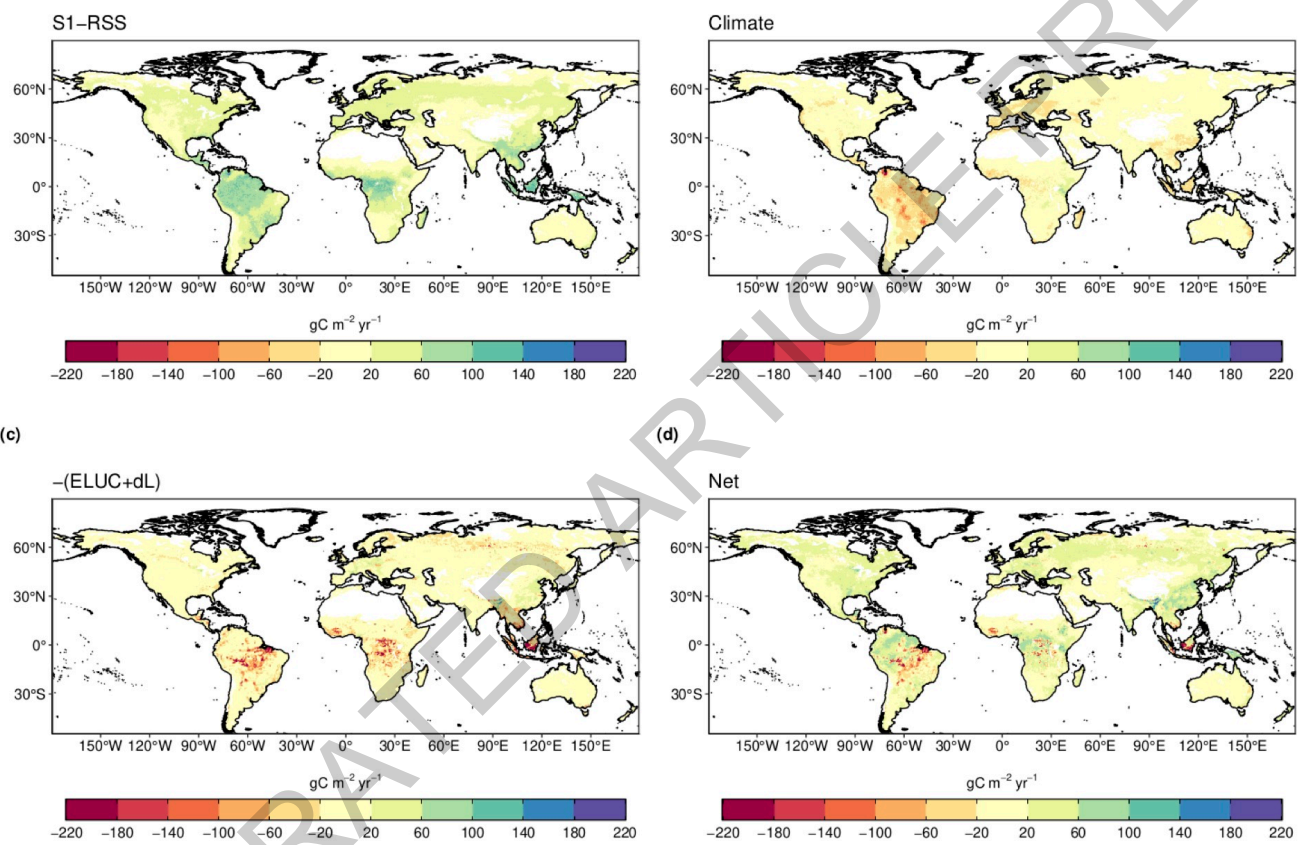
Extended Data Fig. 2



Extended Data Fig. 3



Extended Data Fig. 4



Extended Data Fig. 5

	G_{ATM}	E_{FOS}	E_{LUC}	S_{LAND}	Net Land	S_{OCEAN}	B_{IM}
GCB2024	5.2±0.02	9.7±0.5	1.1±0.7	3.2±0.9	2.1±1.1	2.9±0.4	-0.4±1.3
Revised E_{LUC} δL			1.2±0.7 (+0.1±0.04)	3.2±0.9	2.0±1.1		-0.3±1.3
Revised S_{LAND} RSS				2.75±0.9 (-0.46±0.3)	1.5±1.1		0.1±1.3
Revised S_{LAND} LCE				2.7±0.9 (-0.07±0.06)	1.4±1.1		0.2±1.3
Revised S_{OCEAN}						3.1±0.5 (+0.22±0.23)	-0.02±1.3
This Study	5.2±0.02	9.7±0.5	1.2±0.7	2.7±0.9	1.4±1.1	3.1±0.5	-0.02±1.3
Atmospheric inversions	5.2±0.0	9.7±0.5	N/A	N/A	1.4±0.5	3.1±0.5	0
Atmospheric oxygen	5.2±0.0	9.7±0.5	N/A	N/A	1.0±0.8	3.4±0.5	0

Extended Data Table 1

		1960s	1970s	1980s	1990s	2000s	2014-2023
	E_{FOS}	3.0±0.2	4.7±0.2	5.5±0.3	6.4±0.3	7.8±0.4	9.7±0.5
Net emissions	E_{LUC}	1.6±0.7	1.4±0.7	1.4±0.7	1.6±0.7	1.5±0.7	1.2±0.7
	G_{ATM}	1.7±0.07	2.8±0.07	3.4±0.02	3.1±0.02	4.0±0.02	5.2±0.02
Partitioning	S_{OCEAN}	1.3±0.5	1.6±0.5	2.1±0.5	2.3±0.5	2.5±0.5	3.1±0.5
	S_{LAND}	1.0±0.5	1.7±0.8	1.5±0.8	2.0±0.6	2.4±0.7	2.7±0.9
	B_{IM}	0.5±1.0	0.1±1.2	-0.02±1.2	0.4±1.2	0.3±1.1	-0.1±1.3

Extended Data Table 2